Anomalous volume expansion in $CaRu_{0.85}Fe_{0.15}O_3$: Neutron powder diffraction and magnetic Compton scattering

T. Taniguchi,[1,*] S. Mizusaki,[1] N. Okada,[1] Y. Nagata,[1] K. Mori,[2] T. Wuernisha,[3] T. Kamiyama,[3] N. Hiraoka,[4] M. Itou,[5] Y. Sakurai,[5] T. C. Ozawa,[6] Y. Noro,[7] and H. Samata[8]

[1]*College of Science and Engineering, Aoyama Gakuin University, Fuchinobe, Sagamihara, Kanagawa 157-8572, Japan*

[2]*Research Reactor Institute, Kyoto University, Kumatori-cho, Sennan-gun, Osaka 590-0494, Japan*

[3]*Department of Materials Structure Science, Graduate University for Advanced Studies, Tsukuba, Ibaraki 305-0801, Japan*

[4]*National Synchrotron Radiation Research Center, Taiwan, Hsin-Ann Road, Hsinchu Science Park, Hsinchu 30076, Taiwan*

[5]*Japan Synchrotron Radiation Research Institute (JASRI/SPring-8), Sayo, Hyogo, 679-5198, Japan*

[6]*Nanoscale Materials Center, National Institute for Materials Science, Namiki, Tsukuba, Ibaraki 305-0044, Japan*

[7]*Kawazoe Frontier Technologies Co., Ltd., Kuden, Sakae, Yokohama, Kanagawa 931-113, Japan*

[8]*Faculty of Maritime Sciences, Kobe University, Fukaeminami, Higashinada, Kobe, Hyogo 658-0022, Japan*

(Received 7 June 2006; revised manuscript received 6 November 2006; published 11 January 2007)

Neutron powder diffraction and magnetic Compton scattering measurements were conducted for ferromagnetic $CaRu_{0.85}Fe_{0.15}O_3$ at temperatures between 10 and 300 K. Anomalous volume expansion was observed in the neutron diffraction measurement below the Curie temperature (85 K), and Invar-like behavior was observed below 40 K. However, no structural phase transition was observed down to 10 K. The strong correlation between the volume expansion, ΔV, and the square magnetization, M^2, suggests that the anomalous volume expansion is due to the magnetovolume effect that is caused by the occurrence of ferromagnetism. The magnetic Compton scattering experiments revealed the existence of a magnetic moment on Ru and the antiferromagnetic configuration of Fe and Ru moments. The formation of a ferrimagnetic order through the induction of the magnetic moment on the Ru ion is a possible reason for the anomalous volume expansion observed for $CaRu_{0.85}Fe_{0.15}O_3$.

DOI: 10.1103/PhysRevB.75.024414 PACS number(s): 75.50.Dd, 61.12.−q, 65.40.De, 74.70.Pq

I. INTRODUCTION

Orthorhombic ruthenates, $ARuO_3$ (A=Sr or Ca), have attracted renewed interest since the discovery of superconductivity in Sr_2RuO_4.[1] Although both of these oxides have the same crystal structure and metallic conductivity, they exhibit considerably different magnetism; $SrRuO_3$ is an itinerant ferromagnet with the Curie temperature, T_C, at 160 K,[2–4] whereas $CaRuO_3$ is an itinerant paramagnet.[5,6] In spite of their close crystallographic characteristics, the contrastive magnetic properties between $SrRuO_3$ and $CaRuO_3$ are quite surprising. It is well known that the lattice distortion of $CaRuO_3$ is considerably larger than that of $SrRuO_3$,[7] and the large rotation of the RuO_6 octahedron in $CaRuO_3$ has been considered as a possible reason for the difference in the magnetic properties between $SrRuO_3$ and $CaRuO_3$. The band structure calculation for $ARuO_3$ (A=Sr, Ca) supports the importance of the structural distortion.[8,9] Kiyama *et al.* observed through an x-ray diffraction measurement that the Invar effect occurred in $SrRuO_3$ below T_C.[10] The occurrence of the Invar effect suggests that the 4*d* electrons are itinerant in $SrRuO_3$ and play an important role in causing ferromagnetism, such as that of $ZrZn_2$. On the other hand, $CaRuO_3$ retains the same crystalline structure down to 12 K, and no anomaly was observed in the temperature dependence of the unit-cell volume, suggesting that only the phonon plays a principal role in the thermal expansion of $CaRuO_3$.[11,12]

Recently, it was reported that ferromagnetism occurs in $CaRuO_3$ for a very small substitution of magnetic or nonmagnetic ions to the Ru site.[13–15] In particular, ferromagnetism occurs for a very small substitution (~5%) of iron or manganese ion. Similar ferromagnetic behavior was also observed for the substitution of nonmagnetic ions, such as Rh, Pb, or Sn. These observations suggest that $CaRuO_3$ is an oxide on the verge of the ferromagnetic order. If the ferromagnetism of $CaRu_{1-x}M'_xO_3$ (M'=magnetic or nonmagnetic ions) occurs for the same reason as it does in $SrRuO_3$, it is quite possible that the Invar effect occurs in the ferromagnetic $CaRu_{1-x}M'_xO_3$. In this study, neutron powder diffraction measurements were carried out for $CaRu_{0.85}Fe_{0.15}O_3$ at temperatures between 10 and 300 K using the time-of-flight (TOF) method in order to investigate the relationship between the lattice distortion and the magnetic order. In addition, a Compton scattering experiment was utilized to corroborate our hypothesis.

II. EXPERIMENTAL DETAILS

A polycrystalline specimen of $CaRu_{0.85}Fe_{0.15}O_3$ was prepared by the conventional solid-state reaction method using high-purity powder of $CaCO_3$ (99.9%), Fe_2O_3 (99.9%), and Ru (99.9%). An appropriate amount of the reagents was mixed in an agate mortar, and the mixture was fired at 900 °C in air for 24 h. After the mixture was reground and pelletized, final sintering was performed at 1200 °C for 3 days in air.

The chemical composition and homogeneity of the specimen were characterized by electron-probe microanalysis (EPMA) using wavelength-dispersive spectrometers. Prior to the neutron diffraction measurements, the crystal structure and quality of the sample were examined using x-ray powder diffraction with Cu Kα radiation. Neutron powder diffraction

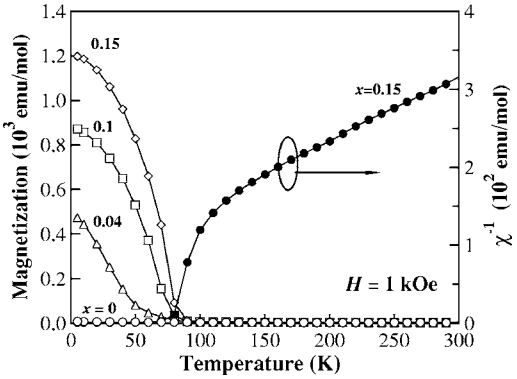

FIG. 1. Temperature dependence of the magnetization measured for $CaRu_{1-x}Fe_xO_3$ (x=0, 0.04, 0.10, 0.15) at 1 kOe and the reciprocal susceptibility, χ^{-1} (solid circles), for $CaRu_{0.85}Fe_{0.15}O_3$.

measurements were carried out using a TOF neutron powder diffractometer (Vega) at the Neutron Science Laboratory (KENS) of the High Energy Accelerator Research Organization (KEK).[16] The diffraction data were collected at temperatures between 10 and 300 K. The structural parameters of $CaRu_{0.85}Fe_{0.15}O_3$ at each temperature were refined using the Rietveld method with the RIETAN-2001T program[17] developed for Vega. The magnetic properties were characterized using a superconducting quantum interface device (SQUID) magnetometer at a temperature range between 5 and 300 K.

The magnetic Compton scattering experiment[18] was carried out at 10 K under an applied field of 2.5 T using the beam line BL08W of SPring-8. The overall momentum resolution was 0.57 atomic units (a.u.: 1 a.u.=1.993 $\times 10^{-24}$ kg m/s). The total spin moment was assigned for the magnetic Compton profile (MCP) by comparing that of an Fe metal standard sample observed at room temperature. The theoretical profiles of the Ru 4*d* and Fe 3*d* electrons were

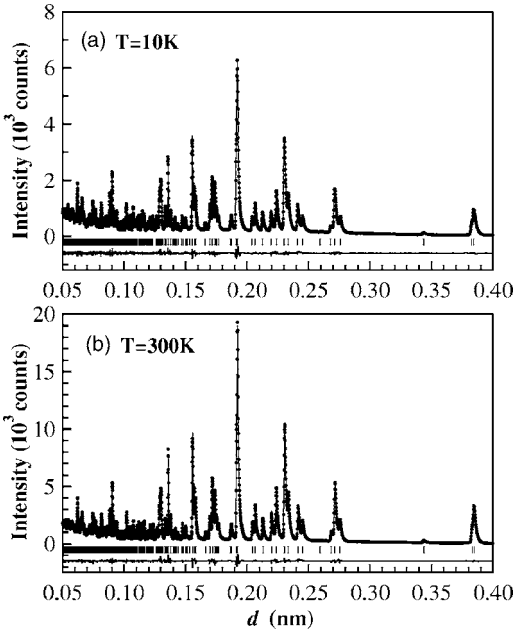

FIG. 2. Neutron powder diffraction profiles and the results of refinement for $CaRu_{0.85}Fe_{0.15}O_3$ at 10 and 300 K. The vertical marks below the profile indicate the positions of Bragg reflections.

obtained by an *ab initio*-restricted Hartree-Fock (RHF) molecular orbital calculation performed for RuO_6 and FeO_6 clusters using the GAMESS program.[19] The structural parameters determined by the present neutron diffraction were used for the calculation.

III. RESULTS AND DISCUSSION

All samples were confirmed to be phase-pure by x-ray powder diffraction. Figure 1 shows the temperature depen-

TABLE I. Results of the Rietveld refinement of the neutron diffraction data obtained for $CaRu_{0.85}Fe_{0.15}O_3$ at 10 and 300 K. B is the isotropic atomic displacement parameter.

T=10 K						
Atom	Site	g	x	y	z	B (Å^2)
Ca	4*c*	1	0.9456(1)	1/4	0.0115(2)	0.214(2)
Ru, Fe	4*b*	1	0	0	1/2	0.036(1)
O(1)	8*d*	1.007(2)	0.2028(1)	0.4534(1)	0.1992(1)	0.230(1)
O(2)	4*c*	0.99(2)	0.0254(1)	1/4	0.5901(2)	0.222(2)
R_{wp}=4.57, R_p=3.55, R_e=3.05, S=1.49, R_I=0.98, R_F=0.56						
T=300 K						
Atom	Site	g	x	y	z	B (Å^2)
Ca	4*c*	1	0.9486(1)	1/4	0.0106(3)	0.651(2)
Ru, Fe	4*b*	1	0	0	1/2	0.259(1)
O(1)	8*d*	1.007(2)	0.2032(1)	0.4546(1)	0.2003(1)	0.516(1)
O(2)	4*c*	0.99(2)	0.0245(1)	1/4	0.5888(1)	0.490(2)
R_{wp}=4.25, R_p=3.18, R_e=2.02, S=2.1, R_I=0.79, R_F=0.54						

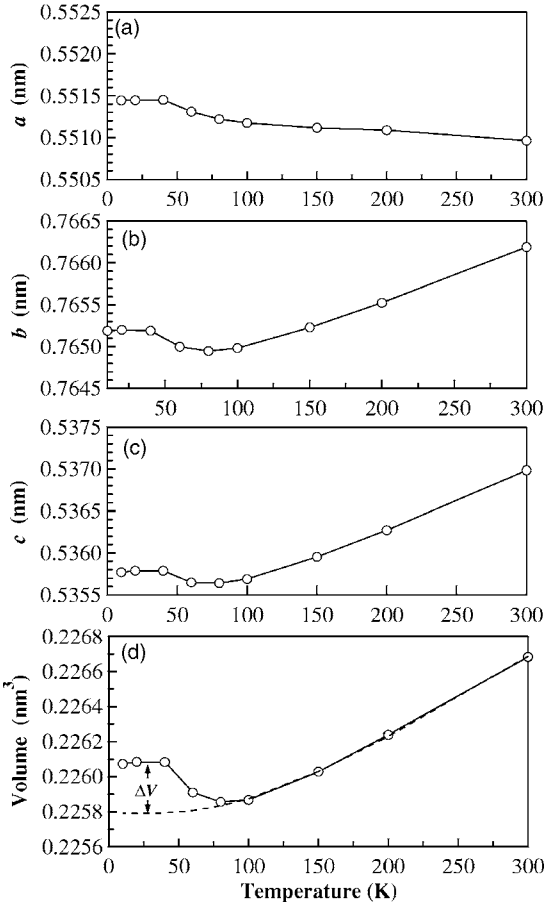

FIG. 3. Temperature dependence of the refined lattice parameters (a) a, (b) b, and (c) c, and (d) unit cell volume obtained for $CaRu_{0.85}Fe_{0.15}O_3$. The dotted line in (d) indicates the unit cell volume calculated by the Debye model. ΔV is the difference between the experimental and the calculated unit cell volumes.

dence of the magnetization measured for specimens of $CaRu_{1-x}Fe_xO_3$ (x=0, 0.04, 0.10, 0.15) under an applied magnetic field of 1 kOe and the reciprocal magnetic susceptibility, χ^{-1}, for the $CaRu_{0.85}Fe_{0.15}O_3$ specimen. When Ru is replaced by Fe, ferromagnetic behavior appears for specimens with an Fe content of $x \geqslant 0.04$. In particular, the magnetization for $CaRu_{0.85}Fe_{0.15}O_3$ shows ferromagnetic behavior with a T_C of 85 K, and the $\chi^{-1}(T)$ shows a ferrimagnetic (parabolic) decrease near T_C as the temperature decreases. Furthermore, the high-temperature portion of the $\chi^{-1}(T)$ can be fitted to the Curie-Weiss law assuming a negative Weiss temperature of −40 K. These results are consistent with those of former studies[15,20] and indicate the ferrimagnetism of $CaRu_{0.85}Fe_{0.15}O_3$.

Figure 2 shows the neutron powder diffraction profiles obtained for $CaRu_{0.85}Fe_{0.15}O_3$ at 10 and 300 K along with the results of refinement for the diffraction data. Both profiles could be refined assuming the orthorhombic $GdFeO_3$-type structure of the space group *Pnma* (No._62). The crystal structure parameters were refined assuming Ca and (Ru, Fe) at the 4c (x,1/4,z) and 4b (0, 0, 1/2) sites, respectively, and oxygen O(1) and O(2) at the 8d (x,y,z) and 4c (x,1/4,z) sites, respectively. In the whole temperature

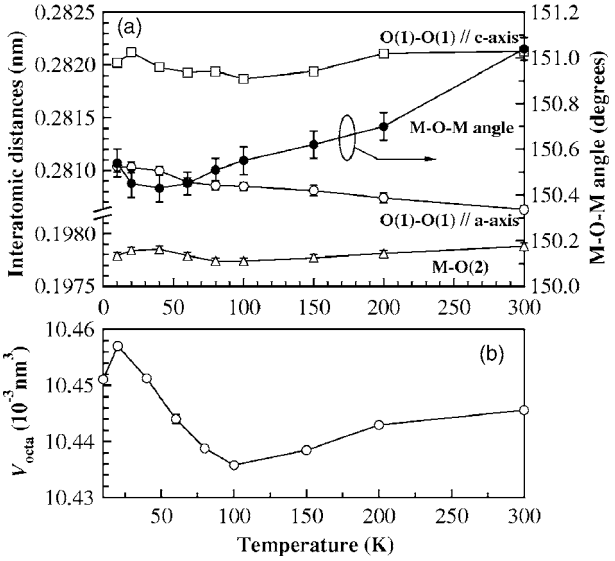

FIG. 4. (a) Interatomic distance between selected atoms and bond angle of M-O-M, where M is Ru or Fe ions. (b) Temperature dependence of the MO_6 octahedron volume.

range, $CaRu_{0.85}Fe_{0.15}O_3$ retained the $GdFeO_3$-type structure, and no structural phase transition was observed. The crystal structure parameters at 10 and 300 K are listed in Table I. The refined occupancy parameters of the oxygen sites indicated that there was no oxygen deficiency at the O(1) and O(2) sites within the standard error. Furthermore, it was revealed that Fe exists as an Fe^{3+} ion in $CaRuO_3$.[19,21] Therefore, the ionic valence is considered to be $Ca^{2+}Ru^{4+}_{0.70}Ru^{5+}_{0.15}Fe^{3+}_{0.15}O^{2-}_3$.

Neutron diffraction measurements were also performed at several temperatures between 10 and 300 K. Figures 3(a)–3(c) show the temperature dependence of the refined orthorhombic lattice parameters a, b, and c obtained for $CaRu_{0.85}Fe_{0.15}O_3$. The lattice parameters b and c decrease with decreasing temperature down to 80 K, whereas parameter a increases as the temperature decreases. These behaviors are similar to those observed in the x-ray powder diffraction measurement for $CaRuO_3$.[15] However, when the temperature is decreased below T_C, parameters b and c increase and become almost constant below 40 K. On the other hand, parameter a continues to increase below T_C and tends to saturate below 40 K. The unit-cell volume calculated from the lattice parameters is shown in Fig. 3(d) as a function of the temperature. In the figure, the dotted line represents the result of fitting using the Debye model that expresses the thermal expansion due to the lattice vibration,

$$V = V_0 + \frac{9\gamma N k_B}{K} T\left(\frac{T}{\Theta_D}\right)^3 \int_0^{\Theta_D/T} \frac{x^3}{e^x - 1} dx,$$

where V_0, γ, N, k_B, K, and Θ_D are the volume at 0 K, the Grüneisen parameter, the Avogadro's number, the Boltzman constant, the bulk modulus, and the Debye temperature, respectively. When V_0=225.8 K and Θ_D=428.6 K were used, the experimental $V(T)$ above 100 K was explained well by this model. However, the experimental $V(T)$ deviates consid-

erably from the calculated unit-cell volume at temperatures below 80 K, which is very close to T_C (85 K) observed in the magnetization measurement. ΔV shows the difference between the experimental unit-cell volume and the unit-cell volume calculated by the Debye model. The unit-cell volume clearly shows anomalous expansion below T_C, and Invar-like behavior is observed below 40 K.

Figure 4(a) gives the interatomic distance between selected atoms and the bond angle of M-O-M, where M is Ru or Fe ions. Figure 4(b) shows the volume of the MO_6 octahedron as a function of the temperature. In the paramagnetic state above T_C, the distance between the transition metal ion and apical oxygen O(2) and the oxygen distance O(1)-O(1) along the c-axis are shortened as the temperature decreases, whereas the distance O(1)-O(1) along the a-axis becomes longer. However, the distances M—O(2) and O(1)-O(1) along the c-axis tend to increase below T_C, while the distance O(1)-O(1) along the a-axis continues to increase regardless of T_C. On the other hand, the bond angle of M-O-M persists to increase beyond T_C as the temperature decreases. The volume of the MO_6 octahedron shows a remarkable increase below T_C. This behavior agrees well with that observed for the unit-cell volume. Since volume expansion occurs below T_C and no structural phase transition has been observed, the occurrence of ferrimagnetism must be the cause of the anomalous expansion. When the anomalous volume effect is due to the occurrence of ferrimagnetism, a strong correlation between ΔV and M^2 (square of magnetization) must be observed.[10] The volume expansion, ΔV, and the M^2 are plotted as a function of the temperature in Fig. 5. The behavior of $\Delta V(T)$ is similar to that of $M^2(T)$ below 80 K, suggesting that the magnetovolume effect due to ferrimagnetism is the cause of the anomalous volume expansion observed for $CaRu_{0.85}Fe_{0.15}O_3$.

When the large magnetovolume effect compensates the thermal expansion due to the lattice vibration, the material shows nearly zero thermal expansion, known as the Invar effect. Some transition metal alloys and weak ferromagnets, such as $ZrZn_2$, are known as substances that show the Invar effect, which is explained in the framework of the SCR theory by considering the band picture and the influence of the spin fluctuation.[22,23] The experimental results of the present study should be treated in the same manner. However, since $CaRu_{0.85}Fe_{0.15}O_3$ is considered as an inhomogeneous system in which Fe ions distribute statistically with the local moment, the model above does not simply apply to our system.

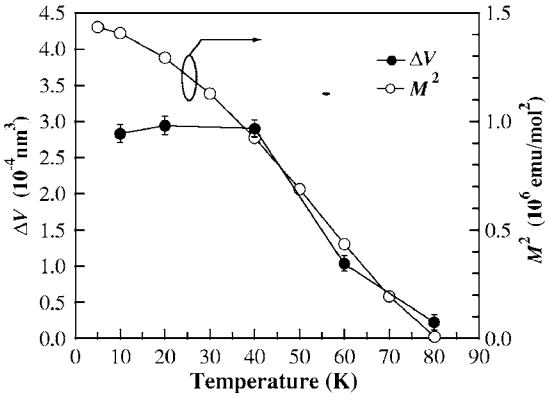

FIG. 5. Temperature dependence of the volume magnetostriction ΔV and the square of the magnetization M^2.

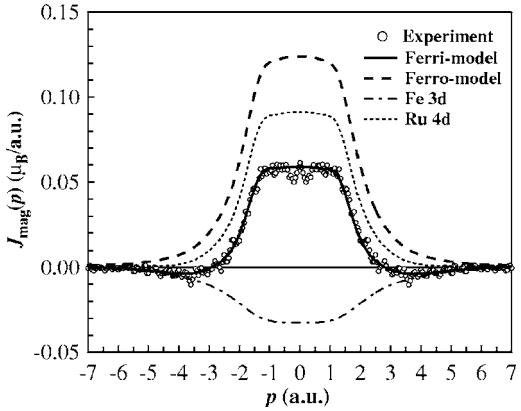

FIG. 6. Experimental magnetic Compton profile (open circle) of $CaRu_{0.85}Fe_{0.15}O_3$ at 10 K under an applied magnetic field of ±2.5 T and best-fit theoretical profile (solid line) based on the ferrimagnetic model. The one-dot chain line and broken line are the atomic profile of Fe and Ru free atoms, respectively. The thick broken line indicates the theoretical magnetic Compton profile based on the ferromagnetic model.

Figure 6 shows the experimental MCP obtained for $CaRu_{0.85}Fe_{0.15}O_3$ at 10 K under an applied magnetic field of ±2.5 T. $J_{mag}(p_z)$ is the one-dimensional projection of the spin-polarized electron momentum density given by

$$J_{mag}(p_z) = \int\int [n\uparrow(p) - n\downarrow(p)]dp_x dp_y,$$

where $n\uparrow(p)$ and $n\downarrow(p)$ are the momentum densities of the majority and minority spin bands, respectively, and the area under the $J_{mag}(p_z)$ is equal to the total spin moment per formula unit.[17] The total spin moment is determined to be 0.20 μ_B by comparing the area under the $J_{mag}(p_z)$ of $CaRu_{0.85}Fe_{0.15}O_3$ with that of the Fe metal standard specimen. The total spin moment is consistent with the moment of 0.20 μ_B obtained by the magnetization measurement. The experimental MCP was decomposed into the profiles of Fe 3d and Ru 4d electrons by the *ab initio* RHF cluster calculation that was used for the analysis of the MCP of $SrRuO_3$.[18,24,25] The calculation was performed for RuO_6 and FeO_6 clusters assuming the valencies of Ca, Ru, Fe, and O as +2, +4, +3, and −2, respectively. The calculated partial RHF Compton profiles for Fe 3d and Ru 4d electrons are shown in Fig. 6. It is clearly seen that $J_{mag}(p_z)$ of 3d electrons has a wider profile than that of 4d electrons, reflecting narrower spatial distribution of 3d wave function. Furthermore, it is recognized that there is no minimum in either profile. In the MCP measurement under an applied magnetic field, the J_{mag} of the electrons with a spin that points in the direction of the applied field has a positive sign, while the J_{mag} of the electrons with an antiparallel spin configuration to the field has a negative sign. As shown in Fig. 6, the experimental MCP has a minimum with a negative value (in the region between

2 a.u. and 5 a.u.). This can be explained when the J_{mag}'s of the 3*d* and 4*d* electrons have an opposite sign and a different spatial extent. As shown in Fig. 6 as the "Ferri model," when the partial spin moments of 0.38 μ_B/f.u. and −0.18 μ_B/f.u. are respectively assigned to the Ru 4*d* and Fe 3*d* profiles and an antiferromagnetic configuration of Ru and Fe moments is assumed, the experimental MCP can be satisfactorily explained. On the other hand, the "Ferro model," which assumes ferromagnetic coupling between Ru and Fe moments, fails to explain the MCP. These results indicate that the Fe spin moment couples with the Ru moment antiferromagnetically and the Ru spin moment makes a dominant contribution to the magnetization, producing a total spin moment of 0.20 μ_B/f.u. for $CaRu_{0.85}Fe_{0.15}O_3$. In that regard, $CaRu_{0.85}Fe_{0.15}O_3$ is considered to be a ferrimagnet.[26,27]

The induction of the magnetic moment on the Ru ion seems to be a possible reason for the ferrimagnetism and the anomalous volume expansion observed for $CaRu_{0.85}Fe_{0.15}O_3$ below T_C. If Ru has a magnetic moment, an Fe ion couples with the six nearest-neighbor Ru ions via a superexchange interaction, forming ferrimagnetic $FeRu_6$ clusters. In a specimen with a small Fe content ($x<0.05$), ferrimagnetic clusters must be localized. However, in $CaRu_{0.85}Fe_{0.15}O_3$, the $FeRu_6$ clusters spread over the crystal, and it is likely that a long-range ferrimagnetic order is established by sharing Ru ions. In ruthenates, the Ru 4*d* orbital forms an antibonding orbital with the O 2*p* orbital, and the antibonding orbital spreads into other Ru ions, forming an antibonding band. In the paramagnetic state, Ru 4*d* electrons preferentially occupy the lower-energy antibonding orbital. However, when ferromagnetism appears and the antibonding band is polarized, Ru 4*d* electrons must occupy the higher-energy antibonding orbital. In this case, the bonding power between Ru and oxygen decreases, resulting in the expansion of the RuO_6 octahedron. Since the anomaly is observed in the temperature dependence of the lattice parameters *b* and *c* at T_C, the easy axis of magnetization seems to be on the *bc* plane. Invar-like behavior was observed at temperatures below 40 K. Although the conclusive reason is presently unclear, this must be due to the fact that the magnetovolume effect approaches saturation at temperatures below 40 K, since the normal thermal expansion is very small at these temperatures.

IV. CONCLUSION

A neutron powder diffraction measurement was performed for ferromagnetic $CaRu_{0.85}Fe_{0.15}O_3$ between 10 and 300 K. The magnetization for $CaRu_{0.85}Fe_{0.15}O_3$ shows ferromagnetic behavior with a Curie temperature T_C of 85 K, and the $\chi^{-1}(T)$ shows a ferrimagnetic (parabolic) characteristic near T_C. Anomalous volume expansion was observed below T_C, and the volume of the $(Ru,Fe)O_6$ octahedron shows a remarkable increase below T_C. This behavior agreed well with that observed for the unit-cell volume. The strong correlation between the volume expansion ΔV and the square magnetization M^2 suggests that the magnetovolume effect is the cause of the anomalous volume expansion. The Invar-like effect was observed below 40 K, and it seems to appear when the magnetovolume effect approaches saturation at very low temperature. The magnetic Compton scattering experiments revealed the existence of a magnetic moment on Ru and the antiferromagnetic configuration of Fe and Ru spin moments. The formation of the magnetic order through the induction of the magnetic moment on the Ru ion is a possible reason for the ferrimagnetism and anomalous volume expansion observed for $CaRu_{0.85}Fe_{0.15}O_3$.

ACKNOWLEDGMENT

The work done at Aoyama Gakuin University was supported by The 21st Century COE Program of the Ministry of Education, Culture, Sports, Science, and Technology, Japan. A part of the work performed at Aoyama Gakuin University was supported by The Private School High-tech Research Center Program of the Ministry of Education, Culture, Sports, Science, and Technology, Japan.

*Corresponding author. Email address:
tk-taniguchi@ee.aoyama.ac.jp

[1] Y. Maeno, H. Hashimoto, K. Yoshida, S. Nishizaki, T. Fujita, J. Bednorz, and F. Lichtenberg, Nature (London) **372**, 532 (1994).
[2] J. M. Longo, P. M. Raccah, and J. B. Goodenough, J. Appl. Phys. **39**, 1327 (1968).
[3] A. Callaghan, C. W. Moeller, and R. Ward, Inorg. Chem. **5**, 1572 (1966).
[4] R. J. Bouchard and J. L. Gillson, Mater. Res. Bull. **7**, 873 (1972).
[5] T. Kiyama, K. Yoshimura, K. Kosuge, H. Michor, and G. Hilscher, J. Phys. Soc. Jpn. **67**, 307 (1997).
[6] G. Cao, S. McCall, M. Shepard, J. E. Crow, and R. P. Guertin, Phys. Rev. B **56**, 321 (1997).
[7] F. Fukunaga and N. Tsuda, J. Phys. Soc. Jpn. **63**, 3798 (1994).
[8] D. J. Singh, J. Appl. Phys. **79**, 4818 (1996).
[9] I. I. Mazin and D. J. Singh, Phys. Rev. B **56**, 2556 (1997).
[10] T. Kiyama, K. Yoshimura, K. Kosuge, Y. Ikeda, and Y. Bando, Phys. Rev. B **54**, R756 (1996).
[11] M. Shepard, S. McCall, G. Cao, and J. E. Crow, J. Appl. Phys. **81**, 4978 (1997).
[12] M. Shepard, P. F. Henning, G. Cao, and J. E. Crow, J. Appl. Phys. **83**, 6989 (1998).
[13] G. Cao, S. McCall, J. Bolivar, M. Shepard, P. Henning, and J. E. Crow, Phys. Rev. B **54**, 15144 (1996).
[14] G. Cao, F. Freibert, and J. E. Crow, J. Appl. Phys. **81**, 3884 (1997).
[15] T. He and R. J. Cava, J. Phys. Condens. Matter **13**, 8347 (2001).
[16] T. Kamiyama, K. Oikawa, N. Tsuchiya, M. Osawa, H. Asano, N. Watanabe, M. Furusaka, S. Satoh, I. Fujikawa, T. Ishigaki, and F. Izumi, Physica B **875**, 213 (1995).
[17] T. Ohta, F. Izumi, K. Oikawa, and T. Kamiyama, Physica B **1093**, 234 (1997).
[18] N. Sakai, J. Synchrotron Radiat. **5**, 937 (1998).
[19] M. W. Schmidt, K. K. Baldridge, J. A. Boatz, S. T. Elbert, M. S.

Gordon, J. H. Jensen, S. Koseki, N. Matsunaga, K. A. Nguyen, S. Su, T. L. Windus, M. Dupuis, and J. A. Montgomery, Jr., J. Comput. Chem. **14**, 1347 (1993).

[20] I. Felner, U. Asaf, I. Nowik, and I. Bradaric, Phys. Rev. B **66**, 054418 (2002).

[21] A. Koriyama, M. Ishizaki, T. Taniguchi, Y. Nagata, T. Uchida, and H. Samata, J. Alloys Compd. **372/1-2**, 58 (2004).

[22] E. P. Wohlfarth, Phys. Lett. **28A**, 569 (1969).

[23] S. Ogawa, J. Phys. Soc. Jpn. **40**, 1007 (1976).

[24] Y. Sakurai, M. Itou, J. Tamura, S. Nanao, A. Thamihavel, Y. Inada, A. Galatanu, E. Yamamoto, and Y. Onuki, J. Phys. Condens. Matter **15**, S2183 (2003).

[25] N. Hiraoka, M. Itou, A. Deb, Y. Sakurai, Y. Kakutani, A. Koizumi, N. Sakai, S. Uzuhara, S. Miyaki, H. Koizumi, K. Makoshi, N. Kikugawa, and Y. Maeno, Phys. Rev. B **70**, 054420 (2004).

[26] S. Mizusaki, T. Taniguchi, N. Okada, Y. Nagata, N. Hiraoka, T. Nagao, M. Itou, Y. Sakurai, T. C. Ozawa, and Y. Noro, J. Appl. Phys. **99**, 08F703 (2006).

[27] S. Mizusaki, T. Taniguchi, N. Okada, Y. Nagata, N. Hiraoka, T. Nagao, M. Itou, Y. Sakurai, T. C. Ozawa, and Y. Noro, Phys. Rev. B **74**, 052401 (2006).